Electrostatically driven long-microbeams for low-frequency applications

A.K. Al-mashaal✉, G. Wood, E. Mastropaolo and R. Cheung

This Letter presents the design, fabrication and characterisation of an array of electrostatically actuated clamped–clamped microbeams. A large bottom actuation electrode and long beams with lengths ranging from 1 to 3.4 mm are the major features of the present device. The novelty of this Letter lies in the realisation of suspended and undeformed microstructures by controlling the process-induced stress during the fabrication process. This has been achieved by compensating the influence of the compressive and tensile stress components of the different deposited layers, resulting in ultralong beams with a relatively straight mechanical profile and an aspect ratio of ~1:3400 of vertical deflection to the beam length. For the first time, ultralong microbeams of tantalum have been actuated electrostatically with AC and DC driving voltages to drive them into resonance and characterise their resonant frequencies. The lowest resonant frequency of 1.4 kHz is obtained for a 3.4 mm-long beam. The shift of the resonant frequency due to the effect of different DC biasing has been investigated experimentally. A spring softening effect has been induced through electrostatic tuning. A downward shift in the resonant frequency to 35,000 ppm for DC bias voltages increasing from 1 to 5 V has been demonstrated.

Introduction: Structures such as beams, plates and membranes are used widely in many micro (MEMS)/nanoelectromechanical systems. In transduction systems, several actuation mechanisms such as electrostatic, electromagnetic, piezoelectric and electrothermal are used to drive these structures where physical or chemical quantities can be sensed or controlled. Electrostatic is the most commonly used actuation mechanism in MEMS devices thanks to its inherent advantages including fast actuation rates, large travel distances, low-power consumption and compatibility with micro-fabrication process. Electrostatically driven MEMS-based clamped–clamped beams have been applied extensively to realise a wide range of transducers for different sensing and actuation applications [1]. From a dynamic performance point of view, however, most of these transducers require high actuation power and operate in a relatively high-frequency regime (up to MHz) as a means to avoid the pull-in instability that takes place when the drive voltage exceeds a certain limit at which the electrostatic force surpasses the elastic force [2]. When the pull-in occurs, the moveable structures undergo a large deformation that may lead to a functional failure and limit the applications of the device. For particular applications such as audio sensors [3], microphones [4], energy harvesters [5], accelerometers [6], low-frequency response is highly desirable. To achieve a proper design of clamped–clamped microbeams that resonate at low frequencies, it is necessary to increase the length or reduce the thickness of the beams. However, the fabrication process for making long suspended beams is extremely challenging. Even for short beams (i.e. length below 500 µm), the effect of stress induced during the deposition and post-fabrication processes can cause the structure to buckle or bend undesirably [7]. In order to realise straight and long suspended beams, the process-induced stress should be controlled, and the aspect ratio of static vertical deflection to beam length needs to be minimised. In our previous study, the influence of stress in tantalum films as a result of deposition and fabrication processes has been optimised [8, 9]. Tantalum has physical and chemical properties such as high melting point, high fracture toughness, and low ratio of Young's modulus to mass density that make it ideally suited for low-frequency applications devices.

In this Letter, we present the design, fabrication and characterisation of an array of electrostatically driven clamped–clamped tantalum microbeams that have a width of 40 µm and a thickness of 1 µm. One of the novelties of the current device lies in its design that includes ultralong-microbeams with lengths ranging from 1 to 3.4 mm. The large aspect ratio (i.e. length to thickness) is the key component of achieving low frequency and high sensitivity of the fabricated structures. Also, our design includes a large bottom actuation electrode that could provide efficient actuation by reducing the driving voltage, hence minimising the pull-in instability. Moreover, the fabrication process has been optimised to enable a successful realisation of fully suspended microbeams without producing geometric deformation such as bending or buckling.

Experimental: Fig. 1 shows the fabrication process flow of the clamped–clamped microbeams. To define the actuation electrode, a lift-off process has been used. First, a photoresist has been spin coated and patterned on an oxidised silicon wafer (Fig. 1*a*). Afterwards, 0.5 µm layer of aluminium metal has been deposited using a DC magnetron sputtering system. Then, the photoresist has been stripped away leaving behind an actuation electrode (Fig. 1*b*). Here, 5.5 µm of polyimide has been used as a sacrificial layer. After coating, the polyimide has been baked initially at 90°C for 90 s and 150°C for a further 90 s. Then, the polyimide has been cured fully at 200°C for 30 min. Chemical mechanical polishing has been employed to planarise the sacrificial layer on the actuation electrode area (Fig. 1*c*). To define the clamped–clamped microbeams, a photoresist has been spin coated and patterned (Fig. 1*d*). Then, a DC magnetron sputtering system has been used to deposit four layers of tantalum using sputtering power of 500 W and sputtering pressure of 20, 10, 20, and 10 mTorr consecutively to form one layer of tantalum of 1 µm thick. As confirmed by curvature measurements, the corresponding residual stress of the deposited tantalum layers will be compressive, tensile, compressive and tensile [8, 9]. In this case, the final residual stress in the whole deposited layer can be compensated by the influence of the compressive and tensile stress component of the different layers. Then, the photoresist has been stripped away and the final structures of clamped–clamped microbeams has been defined (Fig. 1*e*). The final step of the fabrication process is to etch the sacrificial layer using an oxygen plasma-ashing process to release the final structure (Fig. 1*f*). Consequently, an array of clamped–clamped microbeams of tantalum with a thickness of 1 µm, width of 40 µm, and lengths ranging from 1 to 3.4 mm have been fabricated successfully.

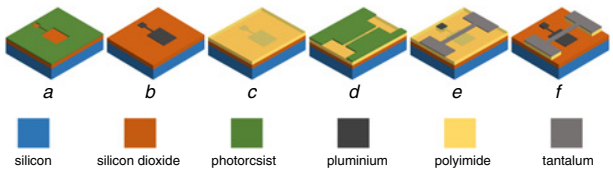

Fig. 1 *Schematic process flow of clamped–clamped microbeams*

a Photoresist spin coated and patterned
b Aluminium deposited, and resist stripped
c Polyimide coated and (chemical mechanical polishing (CMP)) planarized
d Photoresist spin coated and patterned
e Tantalum deposited, and resist stripped
f Polyimide etched, and beams released

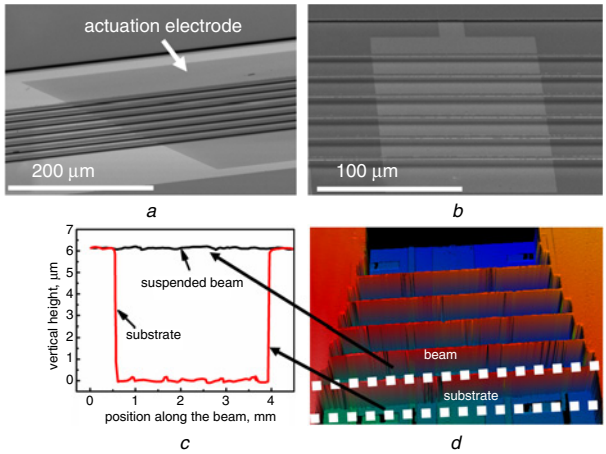

Fig. 2 *Characterisation of clamped–clamped microbeams of tantalum*

a, *b* SEM photographs of the released beams
c, *d* WLI measurement showing the final deflection profile of 3.4 mm-long beam

Characterisation: The fabricated microbeams have been characterised by scanning electron microscope (SEM) and a white light interferometer (WLI, Zygo) to inspect whether the microbeams have been released fully. Fig. 2*a* shows SEM image of an array of the released clamped–clamped microbeams after removing the sacrificial layer with a zoomed-in view in Fig. 2*b*. No upwards or downwards deflection has been observed and it can be seen that the beams are released fully showing a relatively straight profile along the length. Fig. 2*c* shows

the actual profile of the structure while Fig. 2*d* shows a typical WLI measurement of 3.4 mm-long beam suspended over 5.5 µm trench from the substrate. The interferometry image shows a consistent straight profile and the aspect ratio of deflection to the beam length is ~1:3400.

Electrostatic actuation: The resonant frequencies of the fabricated microbeams have been measured by applying an AC harmonic signal (V_{ac}) and a DC voltage (V_{dc}) between the suspended beam and the actuation electrode underneath. In this case, the frequency has swept from 1 Hz to 8 kHz and the first four modal frequencies have been observed. Also, an excitation sinusoidal signal has been applied to measure the amplitude of vibration. The devices have been tested in atmospheric air using a Polytec laser Doppler vibrometer. Fig. 3*a* shows the measurements of the first four modal frequencies of beams with lengths varying from 1 to 3.4 mm. The measurement has been performed while applying 0.5 V of V_{ac} and a 3 V of V_{dc}. It has been observed that the resonant frequency decreases and the amplitude of vibration increases when the beam length increases. For example, the lowest fundamental frequency of 1.4 kHz with an amplitude of ~750 nm has been observed for the longest beams (3.4 mm). In general, the longest beam possesses the lowest frequency and the highest amplitude.

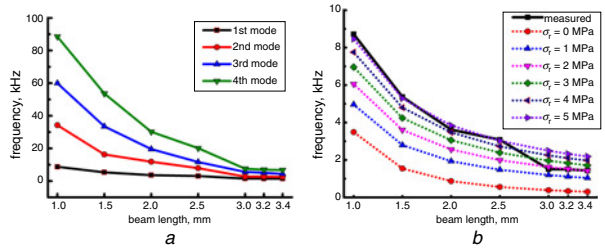

Fig. 3 *Frequency response of tantalum microbeams*

a Measurements of the first four resonant frequencies versus the beams length
b Measurements and FEA simulation of the first resonant frequency using values of stress (0–5 MPa) with respect to the beams length

Although our beams show a straight profile, the stress that might be introduced into the device during the deposition and post-fabrication processes cannot be prevented completely. Therefore, to determine the stress of the fabricated beams, numerical finite-element analysis (FEA) using CoventorWare has been created by applying stress (0–5 MPa). Fig. 3*b* shows the measured (black solid line) and simulated resonant frequencies as a function of the beam length. Since the simulated frequency at 0 MPa (red-dotted line) is lower than the experimental value, most likely the beams are experiencing a tensile stress. By increasing the tensile stress from 1 to 5 MPa, the FEA model shows fairly good agreement with the measurements. Therefore, the tensile stress of our clamped–clamped beams has been estimated to be about 2–5 MPa.

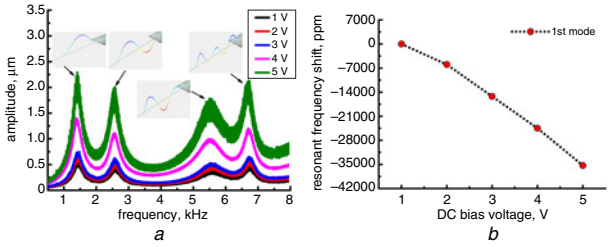

Fig. 4 *Frequency response of 3.4 mm-long microbeam at different tuning voltages. The inset in a shows the corresponding shape of measured modes*

a Measured amplitude of vibration versus resonant frequency for tuning voltages ranging from 1 to 5 V
b Measured resonant frequency shift versus tuning voltage

Frequency tuning: The resonant frequencies of electrostatically driven clamped–clamped microbeams can be tuned by changing the DC voltage across the suspended beam and the actuation electrode. Depending on the excitation voltage, non-linear phenomena such as spring softening and spring hardening can be induced. Fig. 4*a* shows the frequency response of 3.4 mm-long beam to the applied V_{dc} tuning voltage. It can be seen that an increase of the V_{dc} tuning voltage from 1 to 5 V induces spring softening effect. In spring softening, as the oscillation amplitude increases, the effective spring constant decreases and results in a downward shift in the resonant frequency.

A downward shift of the first modal frequency of about −35,000 ppm has been induced when the V_{dc} tuning voltage increases from 1 to 5 V, as depicted in Fig. 4*b*. To avoid pull-in, the beams have been actuated with a small V_{dc} voltage <5 V. Excitation with a higher V_{dc} voltage offset (i.e. higher than 5 V) might introduce non-linearity, and this might explain the noise in the frequency spectrum that has been observed at 5 V. In addition, a significant increase in the amplitude of vibration from about 0.5 to 2.3 µm with the increase of the tuning voltage from at 1 to 5 V.

Conclusions: Long microbeams of length ranging from 1 to 3.4 mm and vertical deflection to beam length aspect ratio of 1:3400 have been realised by controlling the residual stress during the fabrication process. The resonant frequencies of the beams have been characterised experimentally by driving the beams electrostatically. The dependence of the resonant frequency on the beam length and tensile residual stress have been investigated numerically and analytically. The frequency tuning in response to the different DC tuning voltages has been demonstrated. Spring softening effect with a downward shift of the resonant frequency and an increase of the vibration amplitude has been induced in the present structures. Finally, the dynamic behaviour measurements have shown that a low resonant frequency down to 1.4 kHz is achievable with a beam length of 3.4 mm. The implemented device has shown a possibility of operating in a low-frequency regime with high sensitivity, promising practical applications for low-frequency-operated devices.

Acknowledgments: This work was supported in part by Engineering and Physical Sciences Research Council (EPSRC). The Ministry of Higher Education and Scientific Research (MOHESR) of Iraq is acknowledged for the financial support through the PhD scholarship programme.

Submitted: *6 December 2017* E-first: *14 February 2018*
doi: 10.1049/el.2017.4534
One or more of the Figures in this Letter are available in colour online.

A.K. Al-mashaal, G. Wood, E. Mastropaolo and R. Cheung (*School of Engineering, Institute for Integrated Micro and Nano Systems, The University of Edinburgh, Edinburgh EH9 3FF, UK*)

✉ E-mail: asaad.al@ed.ac.uk

References

1 Zhang, W.M., Yan, H., Peng, Z.K., *et al.* 'Electrostatic pull-in instability in MEMS/NEMS: A review', *Sens. Actuat. A Phys.*, 2014, **214**, pp. 187–218
2 Krylov, S., and Dick, N.: 'Dynamic stability of electrostatically actuated initially curved shallow micro beams', *Contin. Mech. Thermodyn.*, 2010, **22**, (6–8), pp. 445–468
3 Chowdhury, S., Ahmadi, M., and Miller, W.C.: 'Design of a MEMS acoustical beamforming sensor microarray', *Sens. J.*, 2002, **2**, (6), pp. 617–627
4 Walser, S., Siegel, C., Winter, M., *et al.* 'MEMS microphones with narrow sensitivity distribution', *Sens. Actuat. A Phys.*, 2016, **247**, pp. 663–670
5 Li, H., Tian, C., and Deng, Z.D.: 'Energy harvesting from low frequency applications using piezoelectric materials', *Appl. Phys. Rev.*, 2014, **1**, (4), p. 41301
6 Liu, H., and Pike, W.T.: 'A micromachined angular-acceleration sensor for geophysical applications', *Appl. Phys. Lett.*, 2016, **109**, (17), p. 173506
7 Fang, W., Lee, C.-H., and Hu, H.-H.: 'On the buckling behavior of micromachined beams', *J. Micromech. Microeng.*, 1999, **9**, (3), pp. 236–244
8 Al-Masha'al, A., Bunting, A., and Cheung, R.: 'Evaluation of residual stress in sputtered tantalum thin-film', *Appl. Surf. Sci.*, 2016, **371**, pp. 571–575
9 Al-masha'al, A., Mastropaolo, E., Bunting, A., *et al.* 'Fabrication and characterisation of suspended microstructures of tantalum', *J. Micromech. Microeng.*, 2017, **27**, (1), p. 15020